Comparison of Raman and Surface FT-IR to Determine the Orientation of α-Synuclein (61-95) in Monolayer

By

Toyin Kenny Akinleye

A Thesis Submitted in Partial Fulfillment of the Requirements for the Degree of Master of Science in Chemistry

Middle Tennessee State University

April 2023

Thesis Committee:

Dr. Chengshan Wang, Chair

Dr. Ngee Sing Chong

Dr. Jing Kong

ACKNOWLEDGEMENTS

I would like to express my profound gratitude to my research advisor Dr. Chengshan Wang for his exceptional guidance and invaluable assistance in my thesis research. I would also like to appreciate my thesis committee Dr. Ngee Sing Chong and Dr. Jing Kong for the time and effort spent in reviewing and providing valuable suggestion towards my thesis work.

I want to sincerely appreciate the MTSU College of Basic and Applied Sciences and the College of Graduate studies for the opportunity provided to pursue my masters and for the graduate teaching assistant which made it possible for me to afford Graduate school. The immense support of the MTSU chemistry department cannot be overemphasized. By providing useful resources and the wealth of knowledge from all the professors has helped me in carrying out chemistry research and improve remarkably. I would also like to specially thank these bodies for their contribution and sponsorship to conferences which has aided my professional development.

In addition, I would like to thank Jessie Weatherly for lending his expertise and assisting with the instrumentation. I want to also appreciate the support and encouragement of my friends.

Finally, I want to appreciate my husband Oluwasoji Akinleye, my mother, Adedoja and my siblings, Fola and Tosin Ajanaku for their prayers, love and support.

ABSTRACT

Membrane proteins poses a lot of challenges for analytical techniques. Thus, it is not a surprise that they are reported to only account for 2.4 % of the solved structures in protein databank, despite being encoded by ~20-30 % of all genes in total genomes. Resolving membrane protein structure is critical because the malfunction of proteins causes many diseases. For instance, the misfolding and subsequent aggregation of alpha-synuclein (α-syn), a protein made up of 140 amino acids, is currently thought to be a main cause of dopaminergic degeneration in Parkinson's disease. An important segmental peptide spanning residues 61-95 also known as the nonamyloid component (NAC) has been detected in the brain of Parkinson disease patients. α-Syn accumulates in the presynaptic terminals where high concentrations of vesicles exist at the amphiphilic interface. However, the reason of the accumulation of α-syn in the presynaptic terminals has been unclear due to the complication of the membrane structure. Fortunately, the amphiphilic membrane structure has been mimicked by the air-water interface as a simple model by a Langmuir monolayer technique. When combined with surface FTIR techniques such as p-polarized multiple-angle incidence resolution spectroscopy (pMAIRS), the conformation and orientation of membrane proteins can be evaluated by deconvoluting the amide I band. In this study, ^{13}C isotope was introduced into α-syn (61-95) at 93G to provide residue-level information. Then, the effect of varying the holding time on the orientation was also investigated. In addition, Raman spectroscopy was also employed in this study and pMAIRS prove to be effective in determining the orientation of α-syn (61-95) even in monolayer.

TABLE OF CONTENT

List of Figures vi

List of Tables viii

List of Schemes ix

CHAPTERS

1. INTRODUCTION 1

1.1 Proteins and Peptides 1

1.2 Methodologies for protein structure 3

1.3 Membrane proteins 4

1.4 α-syn and its segment peptides 5

1.5 Langmuir-Blodgett technique 7

1.6 FTIR and Surface FTIR techniques 8

1.7 p-Polarized Multiple-Angle Incidence Resolution Spectroscopy (pMAIRS) 9

1.8 Previous pMAIRS and Circular Dichroism (CD) results of α-syn (61-95) 10

1.9 ^{13}C Isotope-edited FTIR Spectroscopy 12

1.10 Raman Spectroscopy 13

1.11 Thesis Proposal 15

2. MATERIALS AND METHODS.....16

2.1 Materials 16

2.2 Peptide Synthesis 17

2.3 Mass Spectroscopy 20

2.4 High Performance Liquid Chromatography 21

2.5 Raman Spectroscopy 23

2.6 Langmuir Trough 24

2.7 p-Polarized Multiple-Angle Incidence Resolution Spectroscopy (pMAIRS) 25

3. RESULTS 27

3.1 Raman Spectra 27

3.2 Langmuir Monolayer 30

3.3 pMAIRS results of α-syn (61－95) held at 6 mN/m for 2 hours 32

3.4 pMAIRS results of ^{13}C labeled α-Syn (61－95) held at 6 mN/m for 2 hours 33

3.5 pMAIRS results of ^{13}C labeled α-Syn (61－95) held at 6 mN/m for 15 minutes 34

4. DISCUSSION AND FUTURE PERSPECTIVE.....36

4.1 Discussion 36

4.2 Future Perspective 38

LIST OF FIGURES

Figure 1.1. General structure of an amino acid 1

Figure 1.2. Amino acid structures, names, as well as three-letter and one-letter abbreviations 2

Figure 1.3. Secondary structures of protein 3

Figure 1.4. Langmuir Trough 8

Figure 1.5. In-plane and Out-of-plane vibration modes of pMAIRS 10

Figure 1.6. CD spectra of 0.075 mg/mL α-syn (61-95) dissolved in pure water (dashed line curve) and LB film on quartz slides α-syn (61-95) under 6 mN/m (solid line curve) 11

Figure 2.1. CEM peptide synthesizer 17

Figure 2.2. Wang Resin 18

Figure. 2.3. General scheme of SPPS 19

Figure 2.4. Waters Synapt tandem mass spectrometer with time-of-flight configuration 21

Figure 2.5. HPLC Waters 1525 system 22

Figure 2.6. Lab Ram HR Evolution confocal Raman microscope 24

Figure 2.7. Kibron Langmuir Trough 25

Figure 2.8. Thermo Fischer Nicolet iS50R FTIR 26

Figure 3.1. Raman spectrum of α-syn (57-102) solid sample 28

Figure 3.2. Raman spectrum of aqueous solution sample of α-syn (57-102) 28

Figure 3.3. Raman spectrum of α-syn (57-102) in silver colloid 29

Figure 3.4. Raman spectra of α-syn (57-102) in monolayer 30

Figure 3.5. Stability curves when the Langmuir monolayer of α-syn (61－95) was compressed up to 6mN/m and kept constant for more than 2 hours on pure water subphase. Solid curve is for surface pressure and dashed curve is for molecular area.....31

Figure 3.6. p-MAIRS results of LB film of α-syn (61－95) transferred after the surface pressure was held at 6 mN/m for 2 hours 32

Figure 3.7. pMAIRS results of LB monolayer of the ^{13}C labeled α-syn (61-95) at position 93G transferred at 6 mN/m after the surface pressure was held for 2 hours 34

Figure 3.8. pMAIRS results of LB monolayer of the ^{13}C labeled α-syn (61-95) at position 93G transferred at 6 mN/m after the surface pressure was held for 15 minutes. 35

Figure 4.1. Tilt angle of amide I band (A) 32.2 ^{o} (B) 21.2 ^{o} 36

Figure 4.2. (A) Model of α-helix spinning around its axis at the air-water interface and (B) Backbone carbonyl of α-helix parallel to the interface 37

LIST OF TABLES

Table 1.1. The ^{13}C amide I' band position of various conformations.....13

Table 1.2. The bands position of various secondary structures in Raman spectroscopy in H_2O 14

Table 2.1 lists the materials with the purity and their respective suppliers 16

LIST OF SCHEMES

Scheme 1.1. The sequence of α-syn with N-terminus underlined and C-terminus expressed in italics 6

Scheme 1.2. Illustration pf two probabilities of α-syn (61-96) at the air-water interface .12

CHAPTER 1

INTRODUCTION

1.1 Proteins and Peptides

Critical functions in the body are performed by complex biomolecules and macromolecules known as proteins and peptides. They are made up of one or more extended chains of amino acid (aa) residues bonded together by peptide bonds. While peptides commonly contain between 2 and 50 amino acids, proteins are larger and comprises of more than 50 amino acids. Individual amino acid is made up of one carboxylic acid group, one amino group and a sp3 hybridized α-carbon with varying residues (R-group) as shown in **Figure 1.1**. There are 20 basic amino acids which serve as the building block of proteins and each amino acid can be represented as a single letter, or a triple letter abbreviation as shown in **Figure 1.2.**

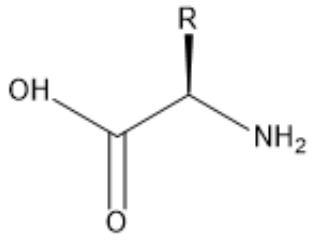

Figure 1.1. General structure of an amino acid.

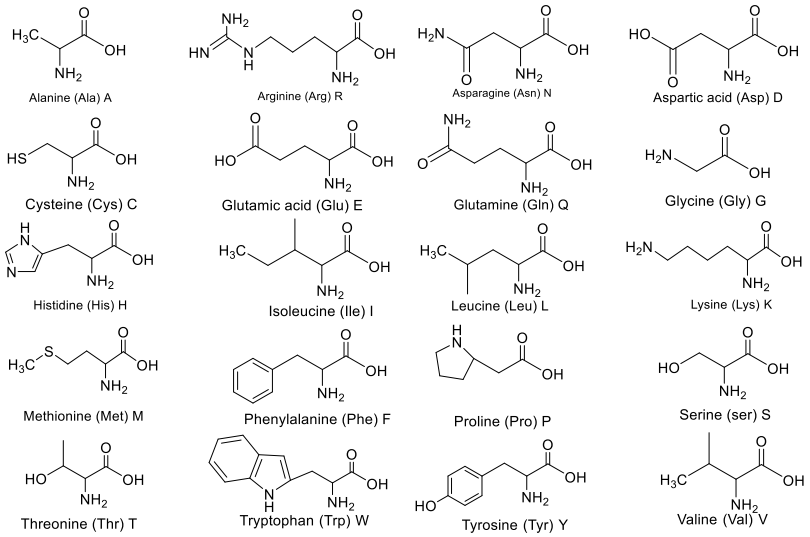

Figure 1.2. Amino acid structures, names, as well as three-letter and one-letter abbreviations.

The way a protein folds into stable three-dimensional structures, or conformations, is determined by its amino acid sequence[1] and the sequence of amino acids in a protein's polypeptide chain is known as its primary structure. The secondary structure of a protein refers to the predictable, recurrent spatial configurations of adjacent amino acid residues in the polypeptide chain.[2] The three secondary conformations typically observed are α-helix, β-sheet, and a random coil[1] as shown in **Figure 1.3**. The various conformations of proteins have been studied using different analytical techniques as understanding protein structure is crucial to understanding their functions. X-ray crystallography and Nuclear Magnetic Resonance (NMR) spectroscopy are the two principal analytical techniques capable of delivering high resolution information about protein structure.

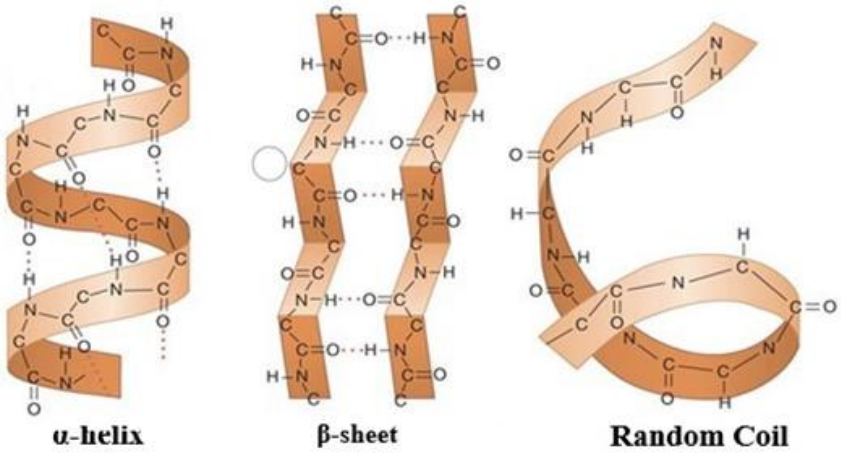

Figure 1.3. Secondary structures of protein.

1.2 Methodologies for protein structure

Nuclear magnetic resonance (NMR) spectroscopy and X-ray crystallography are effective analytical methods for determining the three-dimensional (3D) structure of proteins and peptides at the atomic level.[3] In X-ray crystallography, the target protein is crystallized and exposed to x-ray beams which are diffracted on hitting the crystals. The electron density map necessary for the enhancement and verification of the model structure of the protein is then produced by the diffraction pattern which is dependent on the structure of the lattice.[4] Protein NMR involves the data collection and analysis of an aqueous solution sample of the purified protein placed in a strong magnetic field and conformation is determined from chemical shifts assigned to atoms in the protein molecule. Unfortunately, these techniques are less effective in analyzing membrane proteins as

numerous membrane proteins are incapable of forming the single crystal structure needed for X-ray crystallography.[5, 6] Also, membrane proteins traditionally reside around cell membrane composed of amphiphilic phospholipids bilayer structure which makes it impossible or difficult to acquire NMR spectra due to the slow reorientation of membrane proteins as one of the key factors affecting NMR spectral analyses of proteins is the overall correlation time.[7, 8] In addition, membrane proteins either form transmembrane structures or stay parallel to the surface of the amphiphilic phospholipids bilayer. Regardless of which above-mentioned structure is formed, the natural membrane proteins usually form a monolayer structure around cell membrane/vesicles. Therefore, it is not surprising that membrane proteins only make up 2.4 % of the solved protein databank because neither X-ray crystallography nor NMR can produce high resolution results for proteins in the molecular monolayer structure.[5, 6.]

1.3 Membrane proteins

Membrane proteins are common proteins that interact with or are a part of biological membranes. Irrespective of whether they adhere perpendicular to the surface of the amphiphilic phospholipid bilayer or take the shape of transmembrane structures, the natural membrane proteins often form a monolayer structure around cell membranes or vesicles. Despite being encoded by ~20-30 % of all genes in total genomes, membrane proteins are reported to only account for 2.4 % of the solved structures in protein databank[5, 6] due to the challenges encountered in structural determination using X-ray crystallography and NMR as mentioned previously in **Section 1.2**. Resolving membrane protein structure is critical as the malfunction of proteins causes many diseases. For instance, the misfolding

and subsequent aggregation of alpha-synuclein (α-syn), is currently thought to be the main cause of dopaminergic degeneration in Parkinson's disease.[9]

1.4 α-Syn and its segment peptides

Containing 140 amino acids, α-Syn is a small, naturally unstructured protein[10] shown in **Scheme 1.1.** The primary sequence of α-syn (Scheme 1.1) constitutes three domains:[10] 1) N-terminus domain (aa 1–60), which is a highly conserved, amphiphilic, alpha helix region containing four 11-residue imperfect repetitions of the consensus sequence KTKEGV;[11] 2) the central domain known as the non-amyloid-β component (NAC), (aa 61–95), originally discovered in Alzheimer's disease senile plaques, this area is prone to aggregate and has a high proclivity for forming a beta-sheet conformation. This is a region of interest as a central hydrophobic region corresponding to residues 71–82 was found to be responsible for the misfolding and aggregation of α-Syn into fibrils;[9] 3) C-terminal domain (aa 96-140), negatively charged and rich in acidic residues; 10 glutamates and 5 aspartates, this region is responsible for the disordered structure of α-Syn.[10] In addition, considerable segmental peptides of α-syn have been detected in the lesion region in the PD patients brain.[12] Among the segment peptides, the NAC segment or α-syn (61-95) is an important one.[13] In addition, β-amyloid protein in the senile plaques in the brain of Alzheimer's disease (AD) patients has been found to co-aggregate with α-syn (61-95) in particular.[13]

MDVFMKGLSK AKEGVVAAAE KTKQGVAEAA GKTKEGVLYV GSKTKEGVVH GVATVAEKTK EQVTNVGGAV VTGVTAVAQK TVEGAGSIAA ATGFV*KKDQL GKNEEGAPQE GILEDMPVDP DNEAYEMPSE EGYQDYEPEA*

Scheme 1.1. The sequence of α-syn with N-terminus underlined and C-terminus expressed in italics.

High structural flexibility and the ability to adopt various conformational states in response to its surroundings and interactions characterize α-Syn.[10] It can transform into multiple different conformations, including monomers of α-helical conformation, tetramers, higher-level soluble oligomers, and highly ordered insoluble fibrils of β-sheet conformation.[14] α-syn accumulates in the presynaptic terminals where high concentrations of vesicles exist[15, 16] as a monolayer at the amphiphilic interface. However, the reason of the accumulation of α-syn in the presynaptic terminals has been unclear due to the complication of the membrane structure. Fortunately, the amphiphilic membrane structure has been mimicked by the air-water interface as a simple model, [17, 18] because the accumulation and the interaction between the proteins/peptides molecules at the interface can be precisely monitored by a Langmuir monolayer technique. In addition, surface Fourier Transform Infrared Spectroscopy (FTIR) techniques that can evaluate the conformation and orientation of membrane proteins by amide I band has been developed to resolve this problem when combined with Langmuir monolayer technique. All the techniques are described in detail below.

1.5 Langmuir-Blodgett Technique

Using a device known as a Langmuir-Blodgett trough, the Langmuir-Blodgett technique is used to facilitate the formation of amphiphilic monolayers and thin films at the air/water interface as shown in **Figure 1.4**. Rectangular, the trough has two barriers for compressing the Langmuir monolayer. The trough top is often made of hydrophobic material that improves sub-phase containment and holds the liquid phase where fabrication of monolayers take place. Varying the concentration, proteins are deposited on the surface and distributed evenly throughout the layer and a movable barrier mechanically compresses the two shorter sides of the rectangular surface. The distance between the molecules at the surface can be used to describe area per molecule as both the available surface area and amount of substance deposited on the surface are known. The surface pressure is measured by a pressure sensor/electro balance arrangement, and the area per molecule is obtained from the total area given by the barrier position. As the molecular area decreases, the molecules will be compressed together. This compression results into molecular interactions, which increase the surface pressure of the interface to which the molecules are confined. The surface pressure decreases the surface tension of the liquid due to the presence of the monolayer. The surface pressure-area (π-A) isotherm obtained by compressing the monolayer is the most used character in the description of a monolayer. The increase in surface pressure is detected by an inert probe, which contacts, but does not significantly penetrate the air-water interface. This is accomplished by decreasing the tension it exerts on the mass balance from which it hangs. The orientation of proteins and peptides, expressed by the tilt angle of a vibrational transition moment, as well as information about more detailed structure (such as secondary structure or conformation)

can be determined by combining the Langmuir monolayer approach with surface FTIR techniques,[6] even when the proteins or peptides are in an amphiphilic monolayer.

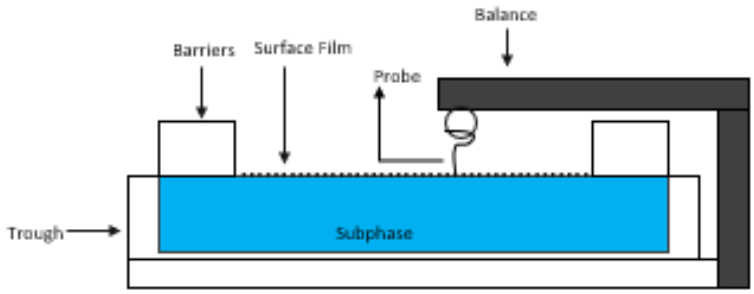

Figure 1.4. Langmuir Trough.

1.6 FTIR and Surface FTIR techniques

A crucial methodology employed in the evaluation of the major secondary structure in a peptide/protein is FTIR spectroscopy.[17] This is achieved by the characteristic peak position of amide I band (from 1600 to 1700 cm^{-1}), which mainly stems from the stretching mode vibration of the backbone carbonyls (i.e., C=O). For example, the amide I band of α-helix is around 1650 cm^{-1}, whereas that of β-sheet is at 1630 cm^{-1}, and that of the unstructured conformation is at 1640 cm^{-1}.[19] A peptide or protein's main conformation can be assessed by deconvoluting the amide I band.[19, 20.]

Generally, surface FTIR techniques include Attenuated Total Reflection (ATR),[6] Infrared External Reflection Spectroscopy (IR-ERS),[17] and p-polarized Multiple Angle Incidence Resolution Spectrometry (pMAIRS).[21] Among these techniques, the available substrates for ATR are limited while the signal of transition moments with tilt angle around the magic angle (i.e., 53.7 º) cannot be detected by IR-ERS.[17] Therefore, IR-ERS can only qualitatively show whether a peptide/protein is roughly parallel or perpendicular to the interface.[17] However, on a number of substrates, including CaF_2 with a low refractive index, pMAIRS can be used to precisely identify the orientation of different vibrations in ultrathin films (even monolayer structure).[21]

1.7 p-Polarized Multiple-Angle Incidence Resolution Spectroscopy (pMAIRS)

pMAIRS, a more modern method, can be used on a lot more substrates than ATR.[21] By decomposing the spectrum to in-plane (IP) spectrum containing vibrations parallel to the interface and out-of-plane (OP) spectrum with perpendicular vibrations (see **Figure 1.5**), the tilt angle of a vibration can be quantitatively determined by **Equation 1** shown:

$$\phi = \tan^{-1}\sqrt{\frac{2A_{IP}}{A_{OP}}} \qquad \text{Equation 1}$$

Where A_{IP} represents the peak area of amide I band in the IP spectrum while the A_{OP} is that of the amide I band in OP spectrum. The tilt angle of the amide I transition moments in relation to the surface is equal to 90º minus ϕ (i.e., 90º - ϕ).

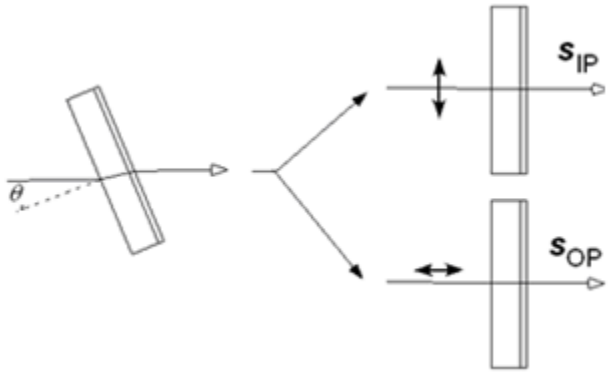

Figure 1.5. In-plane and Out-of-plane vibration modes of pMAIRS.

The conformation or orientation of a particular residue cannot be determined using the standard FTIR approach because it can only produce "low-resolution" results.[22] Nevertheless, the ^{13}C isotope-edited FTIR spectroscopy was recently developed to provide residue level resolution by introducing ^{13}C isotopic labels into the backbone carbonyl (i.e., C=O) of a peptide/protein.[22]

1.8 Previous pMAIRS and Circular Dichroism (CD) results of α-syn (61-95)

At the air-water interface, α-syn and α-syn (61-95) behaved similarly as follows.[23, 24] First, both α-syn and α-syn (61-95) formed a stable Langmuir monolayer at the air-water interface. Secondly, surface FT-IR results showed that both were unstructured in aqueous solution and transformed to α-helical conformation at the interface.[23, 24] In addition, Circular Dichroism (CD) has been used to verify the transformation of α-syn and α-syn (61-95) to α-helix at the interface (**Figure 1.6).**[25] Characteristic peaks of α-helix were detected on the LB films of α-syn (61-95) on quartz slide with two negative peaks at 208 and 221 nm and a positive peak around 190 nm all characteristic of α-helical conformation.[25] This conformation change and

the consequent high stability of the monolayer at the interface may be responsible for the accumulation of α-syn and α-syn (61-95) at the interface.[23, 24] Finally, pMAIRS was shown to be able to quantitatively determine the tilt angle of the axis of α-helical α-syn (61-95) to be 30.1 º.[24]

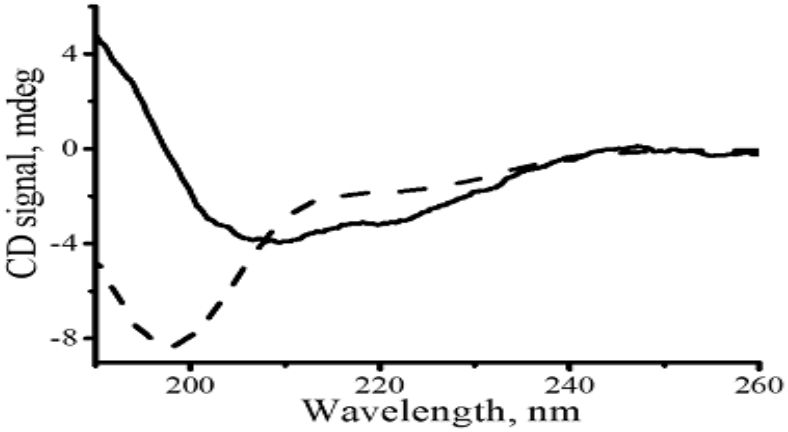

Figure 1.6. CD spectra of 0.075 mg/mL α-syn (61-95) dissolved in pure water (dashed line curve) and LB film on quartz slides α-syn (61-95) under 6 mN/m (solid line curve).

The conformation or the orientation of a specific residue cannot be addressed with traditional FTIR because it can only provide "low-resolution" results.[22] For example, a 0 º tilt angle of a membrane protein means that the protein lies parallel to the membrane whereas a 90 º tilt angle shows that the protein forms a transmembrane structure. Therefore, 30.1 º which is the average tilt angle of the axis at all the thirty-five residues in α-syn (61-95) causes confusions about the behavior of α-syn (61-95) at the interface: will it be parallel to the interface or form transmembrane structure? There are two likely answers to this question as

shown in Scheme 1.2. One possibility is that the axis of all the thirty-five amino acid residues is 30.1 º as shown in Scheme 2A. The other is that the axis of some residues is parallel whereas that of other residues are perpendicular as illustrated in Scheme 2B. The overall tilt angle of Scheme 2B is also around 30.1 º. An approach with higher resolution (such as residue level resolution) is required to address this problem.

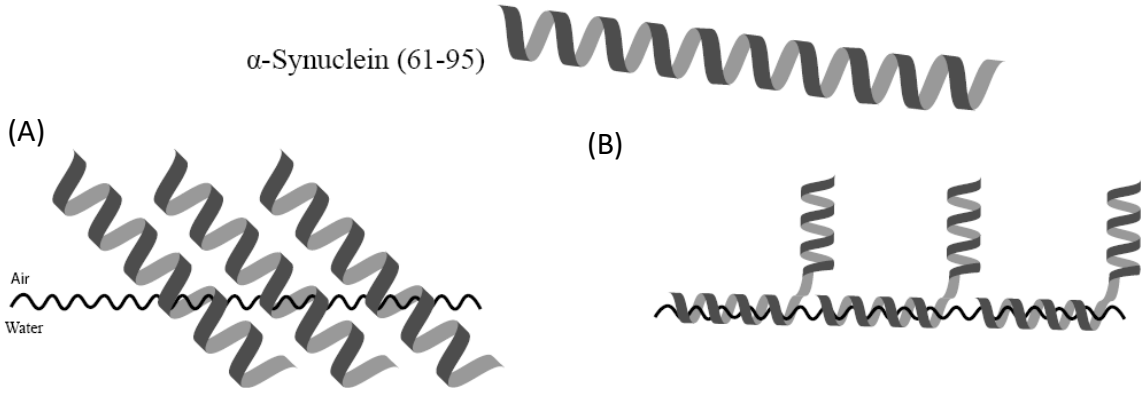

Scheme 1.2. Illustration of two probabilities of α-syn (61-95) at the air-water interface.

1.9 ^{13}C isotope-edited FTIR spectroscopy

By introducing ^{13}C isotopic labels into the backbone carbonyl (i.e., C=O) of a peptide/protein, a technique known as ^{13}C isotope-edited FT-IR spectroscopy has recently been developed to provide residue level resolution.[22, 26] The ^{13}C labeled C=O will generate a ^{13}C amide I band which can provide the conformation of a specific residue.[26, 27] Therefore, it is probable to combine pMAIRS and ^{13}C isotope-edited FTIR to determine the orientation of α-syn (61-95) in residue level even in monolayer. To verify this probability, ^{13}C isotope

was introduced into the backbone carbonyl of 93G at the C-terminus of α-syn (61-95). The ^{13}C amide I band was only detected in the S_{IP} and disappeared in S_{OP}. This verified that the axis of the α-helix of α-syn (61-95) at 93G is almost 0 º to the surface as shown in Scheme 1.2 above. However, there is challenge of the overlap of the ^{13}C amide I' band of α-helix and β-sheet due to coupling (i.e., ^{13}C-^{13}C and ^{13}C-^{12}C coupling), **Table 1.1** summarizes the overlapping issue. The overlapping makes it difficult to distinguish the α-helix and β-sheet conformation. Fortunately, this overlapping issue can be resolved by Raman spectroscopy.

Table 1.1. The ^{13}C amide I' band position of various conformations

Secondary structures	Unstructured conformation	α-helix	Anti-parallel β-sheet	
			^{13}C-^{12}C coupling	^{13}C-^{13}C coupling
Position of ^{13}C amide I band	Not detectable	1590~1599 cm^{-1}	1600 cm^{-1}	1590 cm^{-1}

1.10 Raman Spectroscopy

Raman spectroscopy is another method that can be used to determine the structure of proteins and peptides.[28, 29] In Raman spectroscopy of proteins/peptides, there are four major amide bands: amide I band, amide II band, amide III band, and C_α–H_b band as shown in

Table 1.2. Like FT-IR, the amide I band is related to the C=O stretching, and amide II band is associated with N–H bending mode in Raman. The C_{α}–H_b band correlates primarily with the bending mode of C_{α}–H. Particularly, the amide III band in Raman spectroscopy is attributed to the C–N stretching in the backbone amide bond and the position of the amide III band is only related to the conformation of local amide bond without any coupling. Therefore, the amide III band in Raman spectroscopy can be used to resolve the above-mentioned overlapping issue in FT-IR spectroscopy.

Table 1.2. The bands position of various secondary structures in Raman spectroscopy in H_2O.

Raman bands	Random coil	α-helix	β-sheet
amide I band position	~1665 cm^{-1}	~1647 cm^{-1}	~1654 cm^{-1}
amide II band position	~1560 cm^{-1}	~1545 cm^{-1}	~1551 cm^{-1}
amide III band position	~1267 cm^{-1}	~1299 cm^{-1}	~1235 cm^{-1}
C_{α}–H_b band position	~1386 cm^{-1}	Not available	~1386 cm^{-1}

1.11 Thesis proposal

As previously mentioned, isotopic labeling of the backbone carbonyl (i.e., C=O) of a peptide/protein provides residue level resolution that can give the conformation of specific residues. Also, it was reported that biophysical behavior (such as conformation and orientation) of residues close to the terminus might be different to the behavior of those in the middle of the sequence.[27] The goal of this thesis is to isotopically label the backbone carbonyl of the NAC region of α-syn (α-syn 61-95) at different positions to investigate the conformation and orientation of specific residues by pMAIRS, to provide residue-level resolution for membrane proteins existing in monolayer form. In addition, some key details (such as surface pressure and holding time) which may affect the orientation will be also studied. Finally, Raman spectroscopy will be used to resolve the spectral overlapping issue in FTIR.

CHAPTER 2

MATERIALS AND METHODS

2.1 Materials

Table 2.1 lists the materials with the purity and their respective suppliers.

Materials	% Purity	Suppliers
Piperidine	99.00	Sigma-Aldrich (St. Louis MO)
Fmoc-Asparagine	99.69	Chem-Impex Int'l (Wood Dale IL)
Fmoc-Alanine	99.91	Chem-Impex Int'l (Wood Dale IL)
Fmoc-Glutamine	99.61	Chem-Impex Int'l (Wood Dale IL)
Fmoc-Glutamic acid	99.11	Chem-Impex Int'l (Wood Dale IL)
Fmoc-Glycine	99.37	Chem-Impex Int'l (Wood Dale IL)
Fmoc-Isoleucine	> 98.00	Novabiochem (Hohenbrunn, Germany)
Fmoc-Leucine	99.80	Chem-Impex Int'l (Wood Dale IL)
Fmoc-Lysine	99.84	Chem-Impex Int'l (Wood Dale IL)
Fmoc-Serine	99.83	Chem-Impex Int'l (Wood Dale IL)
Fmoc-Threonine	99.60	Novabiochem (Hohenbrunn, Germany)
Fmoc-Valine	99.53	Novabiochem (Hohenbrunn, Germany)
Hydroxybenzoyltriazole (HOBT)	> 99.00	Anaspec Inc. (Fremont, CA)
Wang Resin	> 99.00	Novabiochem (Hohenbrunn, Germany)
Dichloromethane (DCM)	99.60	Fisher Scientific (Fairlawn, NJ)
Acetonitrile	99.90	Fisher Scientific (Fairlawn, NJ)
N,N-dimethylformamide (DMF)	99.80	Fisher Scientific (Fairlawn, NJ)
Diethyl ether	99.90	Fisher Scientific (Fairlawn, NJ)
4-dimethylaminopyridine (DMAP)	≥ 99.00	Fisher Scientific (Fairlawn, NJ)
Triisopropysilane (Tis)	98.00	Sigma-Aldrich (St. Louis, MO)
Trifluoroacetic acid (TFA)	99.00	Alfa Aesar (Ward Hill, MA)
Diisopropylcarbodiimide (DIC)	99.00	Anaspec Inc. (Fremont, CA)
Nitrogen gas	99.99	NexAir (Memphis, TN)
Silicon wafer		University Wafer Inc. (Boston MA)
Silver nitrate	99.9	Alfa Aesar (Ward Hill, MA)
Sodium citrate	≥ 99.00	VWR Chemicals (Solon, OH)

2.2 Peptide Synthesis

Figure 2.1. CEM peptide synthesizer.

The peptides examined in this thesis were synthesized in the lab using a CEM peptide synthesizer as depicted in **Figure 2.1** via Solid Phase Peptide Synthesis (SPPS). SPPS involves synthesizing the target peptide on an insoluble solid support polymer and growing peptides from the C-terminus to the N-terminus. Here, the solid support is Wang resin, shown in **Figure 2.2** which has good swelling, mechanical strength, and stability. Also, in moderately acidic conditions, the resin can be cleaved efficiently, as well as the deprotection of side chain protecting groups. The amine group of individual amino acid is protected by fluorenylmethyloxycarbonylchloride (Fmoc) chemistry. In this protection strategy, Fmoc group is used to protect the amine group of each amino acids to prevent

solution coupling of dissolved amino acids and the side chains of amino acids are protected with base-stable protecting groups such as tert-butyloxycarbonyl (Boc) and t-butyl (tBu).

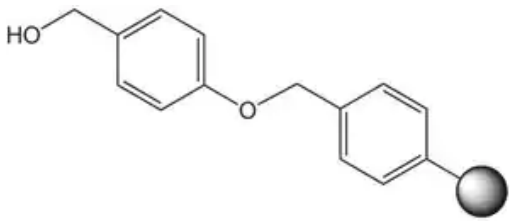

Figure 2.2. Wang Resin.

As demonstrated in **Figure 2.3**, SPPS entails the repeated stages of coupling-washing-deprotection-washing. The C-terminal of the first Fmoc protected amino acid was attached to Wang resin (solid support) by using DMAP to catalytically accelerate the activation of the amino acid carboxyl and 0.2 molar equivalents of Wang resin. DIC and HOBt were added to activate the carboxylate and decrease racemization, respectively. Reaction between the activated carboxylate and the amine group of solid support results in an amide bond. The resin was subsequently cleaned by using DMF three times, as well as the surface of the solid phase.

The amine group is then deprotected by eliminating Fmoc using 1:4 (v/v) piperidine/DMF. The amino acid is now exposed and ready to couple with the subsequent

amino acid as a result. The process is then finished by repeatedly washing with DMF. The first amino acid becomes linked to the solid support and the next amino acid was prepared and added to the growing chain. This coupling-washing-deprotection-washing sequence was repeated until desired amino acids were all coupled. Once desired sequence is achieved, the peptide was cleaved from the resin by first washing with DCM followed by suspending in a solution of 75 % TFA, 22 % DCM, 1.5 % TIS, and 1.5 % H_2O, intermittently shaking the solution to break the bond between the peptides C-terminal carboxylic group and the resin. TFA deprotects side chains removing the protecting groups such as Boc and tBu, addition of H_2O and TIS prevents side reactions during the side chain deprotection stage. DCM, TIS, TFA and H_2O was removed by purging with nitrogen. After the addition of diethyl ether, the peptide was centrifuged and the liquid was decanted, leaving the crude product of synthetic peptide.

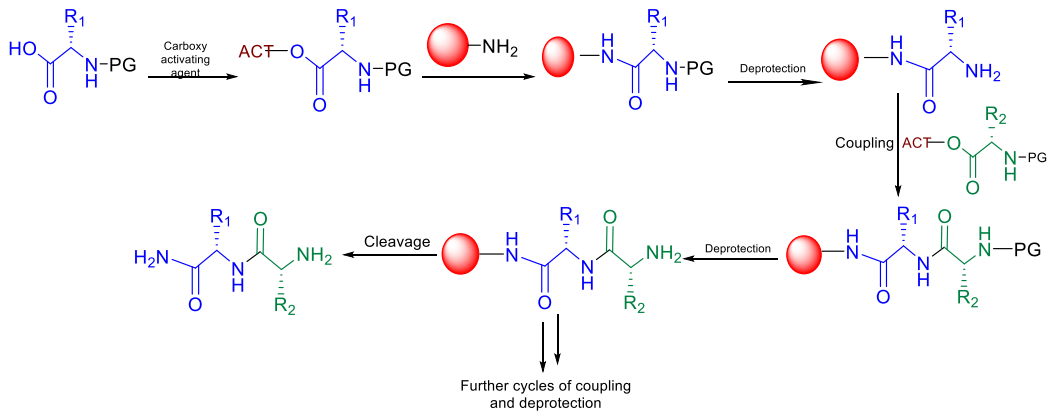

Figure. 2.3. General scheme of SPPS.

2.3 Mass Spectroscopy

Mass Spectroscopy (MS) is an analytical technique employed in the identification of a vast array of chemical compounds. It measures the mass to charge ratio of molecular ions generated by the ionization of the chemical compounds in the sample and it is used to ascertain the chemical structures, elemental composition, and molecular mass of a sample. A mass spectrometer consists of three major components: the ion source, which facilitates the conversion of the sample into ions; the mass analyzer, which separates the ions of various molecules according to their mass-to-charge ratios; and the detector, which measures the signal intensities for the quantitative determination of ion abundances in the sample.

A Waters SYNAPT q-TOF tandem mass spectrometer equipped with an electrospray ionization (ESI) and atmospheric pressure chemical ionization (APCI) ion sources shown in **Figure 2.4**, was utilized for all mass spectrometric measurements performed in this thesis. A small sample of the peptide was completely dissolved in water before it was injected into the MS with a 500 μL syringe. The positive ion mode of ESI was used for MS measurements with capillary ionization voltage set to 3.00 keV and sample cone temperature at 150 °C. N_2 gas was used for desolvation and kept at a flow rate of 500 L/hour. A mass spectrum was produced with a plot of the mass-to-charge ratio against intensity.

Figure 2.4. Waters Synapt tandem mass spectrometer with time-of-flight configuration.

2.4 High performance liquid chromatography

All proteins synthesized in this thesis were purified by high performance liquid chromatography (HPLC). The HPLC instrument makes use of a chromatographic column packed with porous materials and compounds are separated based on how well they bind to the surface of the porous materials. **Figure 2.5** displays a Waters 1525 Binary Solvent Pump (Waters Corp., Milford, MA), attached to a Phenomenex Reverse Phase Semi Prep C18 Column, Jupiter Model 00G-4055- P0 with column dimensions of internal diameter of 21.5 mm and length of 250 mm (Phenomenex, Inc. Torrence, CA) where protein purification was conducted. Detection was conducted by a Waters 2489 UV-Vis detector

(Waters Corp., Milford, MA), at UV absorption wavelength of 250 nm. Mobile phase A was a solution of ultra-pure water with 0.1 % TFA (v/v), and mobile phase B was a solution of HPLC grade acetonitrile with 0.1 % TFA (v/v). Separation was carried out by using a linear gradient of 8 % to16 % by volume of A and (92 % to 84 % of B at a flow rate of 21.5 mL/minute for 50 minutes. When the target peptide's molecular weight was validated and the retention time of the peptide was determined by MS, the purifying method was repeated for the crude products. The purified fractions were then collected and frozen at -80 °C before being lyophilized to produce the pure solid peptide.

Figure 2.5. HPLC Waters 1525 system.

2.5 Raman Spectroscopy

Peptides were measured by Raman Spectroscopy using a Lab Ram HR Evolution confocal Raman microscope with a 532 nm excitation laser as shown in **Figure 2.6**. For α-syn (57-102), Raman spectra of the solid peptide was obtained, followed by the aqueous solution, aqueous solution peptide in colloidal silver, and peptide monolayer. Throughout data collection, the grating was set at 600 grooves/mm and the objective of the microscope used was at 50x using the_VIS_LWD objective. The Raman spectra of α-syn (57-102) in pure solid and the solution peptide in silver colloid were obtained using an aperture of 1000, an acquisition time of 5 seconds, accumulation set at 10, and ND filter set at 100 %. While the spectra of the aqueous solution of peptide as well as peptide monolayer were collected using an aperture of 200, at acquisition time of 10 seconds, accumulation set at 20 and ND filter set at 100 %.

Silver colloidal solution was employed in Surface-enhanced Raman Spectroscopy (SERS). It was prepared by boiling 90 mg of silver nitrate dissolved in 500 ml bidistilled water after which 114 mg of sodium citrate dissolved in 10 ml bidistilled water was added dropwise and mixture boiled under vigorous stirring for 90 min to reduce the silver cations into silver nanoparticles. [30]

Figure 2.6. Lab Ram HR Evolution confocal Raman microscope.

2.6 Langmuir trough

A Kibron µtrough Langmuir trough XS (Kibron Inc., Helsinki Finland) was used to examine the stability of the surface pressure-area (π-A) isotherm of the Langmuir monolayer of α-syn (61-95) on pure water subphase and the deposition of its LB film to silicon slides as shown in **Figure 2.7**. The concentration of α-syn (61-95) aqueous solution was 1.5 mg/mL and using a 25 µL syringe (Hamilton Inc., Reno, Nevada) held less than 1 cm from the subphase surface, 25 µL of α-syn (61-95) was spread at the air-water interface, followed by a 30-min period for the formation of monolayer. The α-syn (61-95) Langmuir monolayer was transferred to the silicon wafer under the surface pressure of 6 mN/m to make the Langmuir-Blodgett films of α-Syn (61-95). The silicon wafer was moved slowly at 0.3 cm/minute after it was held at varying times before transference.

Figure 2.7. Kibron Langmuir Trough.

2.7 p-Polarized Multiple-Angle Incidence Resolution Spectroscopy (pMAIRS)

Using a Thermo Fisher Scientific Nicolet iS50R FT-IR spectrometer equipped with a pMAIRS accessory as shown in **Figure 2.8**, pMAIRS was performed by putting the LB film monolayer on the silicon (Si) substrate in the pMAIRS accessory and transmitting IR beam through the sample. The refractive IR beam was directed onto the HgCdTe (MCT-A) detector. With a modulation of 50 kHz, the bare Si substrate was used as the background for measuring the spectra of a-syn (61－95) sample. The spectra of both background and sample were acquired over nine thousand scans at a resolution of 8 cm^{-1}. Based on all the background and sample results of various incident angles from 9 º to 44 º, the in-plane (IP) and out-of-plane (OP) spectra were calculated. The following equation was used to determine the orientation angle of the amide I band with respect to the surface normal (i.e., in Equation 1):

$$\phi = \tan^{-1}\sqrt{\frac{2A_{IP}}{A_{OP}}} \qquad \textbf{Equation 1}$$

Where A_{IP} represents the peak area of amide I band in the IP spectrum while the A_{OP} is that of the amide I band in OP spectrum. The tilt angle of the amide I transition moments in relation to the surface is equal to 90 º minus ϕ (i.e., 90 º - ϕ).

Figure 2.8. Thermo Fisher Nicolet iS50R FTIR.

CHAPTER 3

RESULTS

3.1 Raman spectra

The Raman spectrum of the pure solid sample of α-syn (57－102) displays a distinct amide I band peak observed at ~1670 cm^{-1} and amide III band peak observed at ~1226 cm^{-1} as shown in **Figure 3.1.** These bands are important in identifying the conformation of peptides. The spectrum also displays the amide II and Cα-H_b peaks observed at ~1546 cm^{-1} and ~1448 cm^{-1} respectively. Since peptides exists as solutions in the body, α-syn (57－102) was studied in solution and its Raman spectrum is displayed in **Figure 3.2.** This spectrum is similar to **Figure 3.1,** except that the amide I band is suppressed, and the amide III band is absent. Although the reason for this phenomenon is still unclear, silver colloid was added to the aqueous solution of the peptide to resolve this problem.

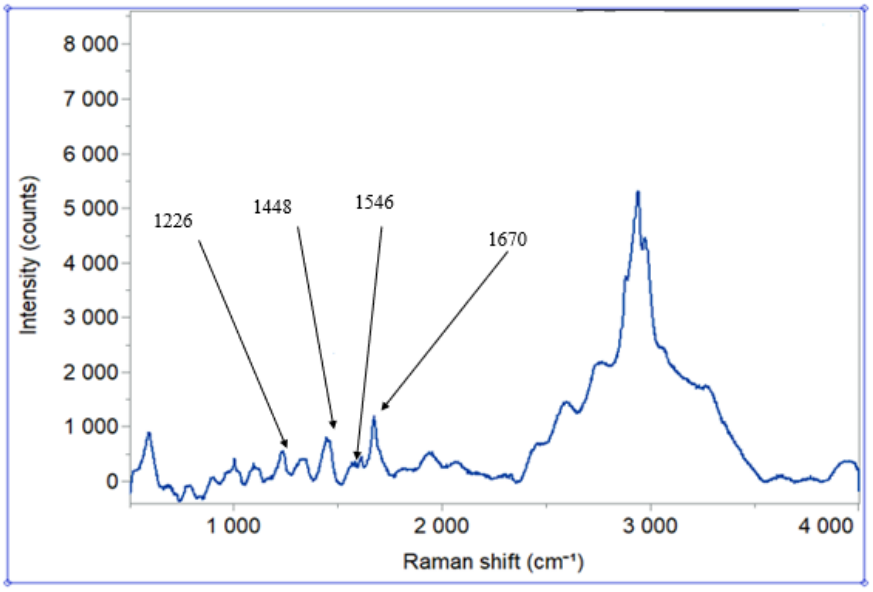

Figure 3.1. Raman spectrum of α-syn (57－102) solid sample.

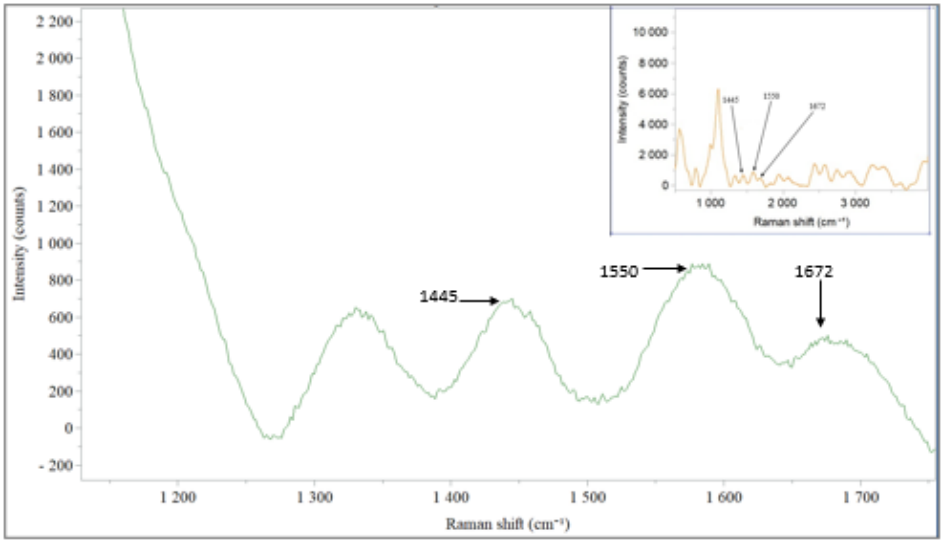

Figure 3.2. Raman spectrum of aqueous solution sample of α-syn (57－102).

In colloidal silver, the aqueous solution of α-syn (57－102) produced a Raman spectrum with a slightly improved amide I band peak observed at ~1669 cm^{-1} as shown in **Figure 3.3,** but this band is still not strong enough. Because α-syn is a membrane protein, it is important to study the peptide in monolayer. **Figure 3.4** displays the Raman spectrum of α-syn (57－102) monolayer where the only peak observed is the signal from silicon wafer. Since a long spectral acquisition time will be needed to yield useful signals, FTIR measurements were conducted on the α-syn monolayer.

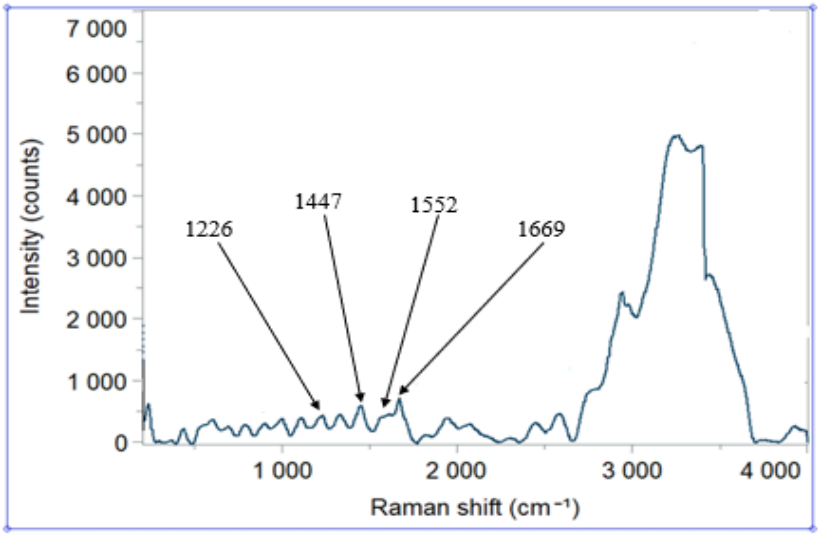

Figure 3.3. Raman spectrum of α-syn (57－102) in silver colloid.

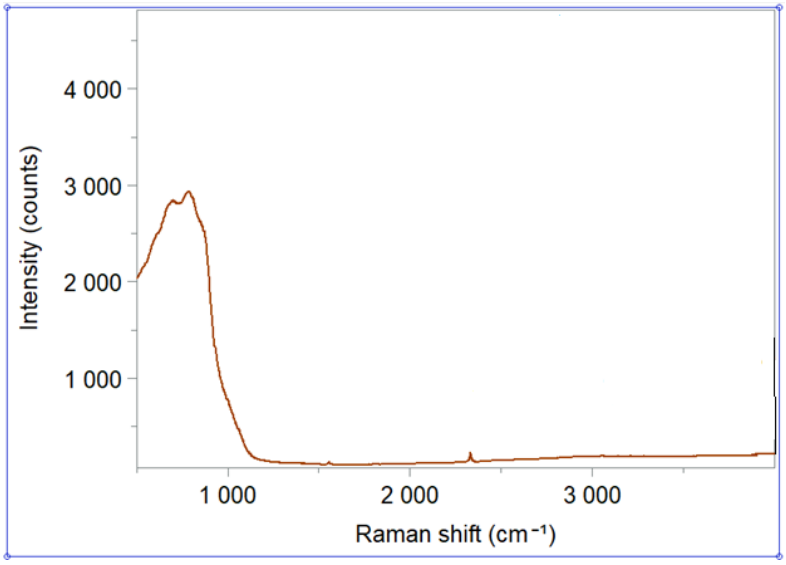

Figure 3.4. Raman spectrum of α-syn (57－102) in monolayer.

3.2 Langmuir Monolayer

α-syn (61－95) forms a stable Langmuir monolayer as indicated in **Figure 3.5**. The α-syn (61－95) Langmuir monolayer was compressed to a surface pressure of 6 mN/m and the surface pressure was kept constant over two hours. The surface pressure (solid line curve) and area (dashed line curve) were monitored over the entire experiment. With increasing surface pressure from 0 to 6 mN/m, there was also a decrease in area. Within the first 45 minutes, the molecular area noticeably reduced after reaching 6 mN/m. After that, the molecular area decreased only less than 1 % even after 2 hours compression. This indicates that the orientation of α-syn (61－95) may be different under various holding time at 6 mN/m. pMAIRS was used to analyze the orientation of α-syn (61－95) for 15

mN/m in our previous publication and the tilted angle is 32.2 °. Here, we continued to study the orientation when the monolayer was held at 6 mN/m for 2 hours and the results are below.

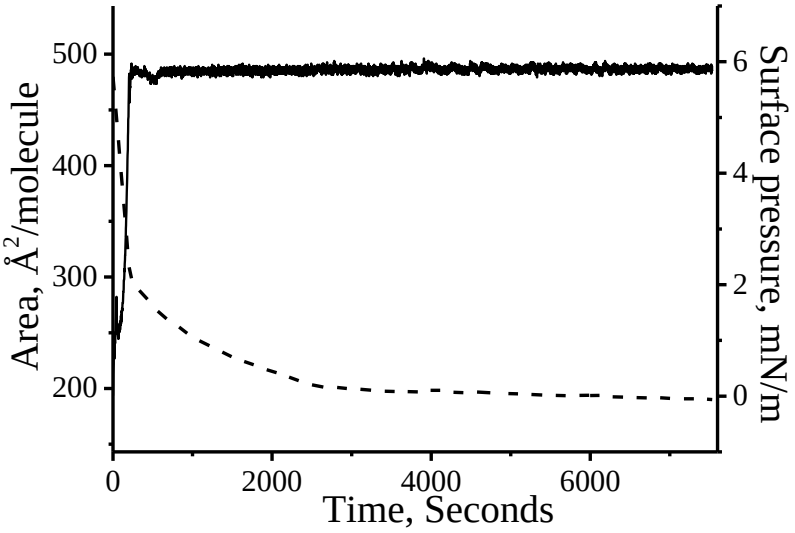

Figure 3.5. Stability curves when the Langmuir monolayer of α-syn (61 ─ 95) was compressed up to 6 mN/m and kept constant for more than two hours on pure water subphase. Solid curve is for surface pressure and dashed curve is for molecular area.

3.3 pMAIRS result of α-Syn (61－95) held at 6 mN/m for 2 hours.

The pMAIRS result containing IP and OP spectra of the LB monolayer of α-syn (61－95) held at 6 mN/m for 2 hours is shown in **Figure 3.6**. The peak position of amide I band in both IP and OP spectra is at 1658 cm^{-1} which is the characteristic peak of α-helix. According to Equation 1 described in Chapter 1 and 2, the tilted angle of amide I band is 21.2 °, which is lower than that (i.e., 32.2 °) held for only 15 minutes. The decreasing titled angle means a more parallel orientation of the axis of α-helix in the monolayer. To double check the orientation of specific residues, ^{13}C isotope label has been introduced into the sequence of α-syn (61－95) and was studied by pMAIRS to address the orientation change of specific residues under various holding time.

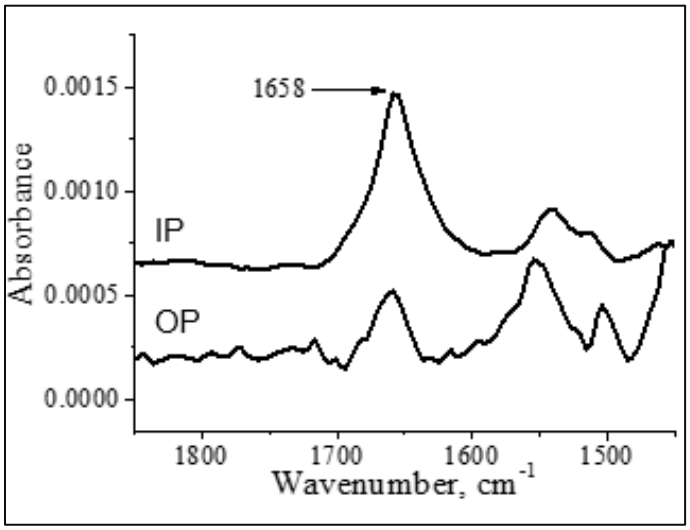

Figure 3.6. p-MAIRS results of LB film of α-syn (61－95) transferred after the surface pressure was held at 6 mN/m for 2 hours.

3.4 pMAIRS results of ^{13}C labeled α-Syn (61－95) at 93G held at 6 mN/m for 2 hours

^{13}C label was introduced into the sequence of α-syn (61－95) at 93G and **Figure 3.7** shows the pMAIR results of its LB monolayer transferred after the monolayer was held at 6 mN/m for two hours. The in-plane (IP) spectrum of the ^{13}C labeled α-syn (61-95) is shown as the top curve in **Figure 3.7**. Similar to that of unlabeled α-syn (61-95) published before,[23] both regular amide I and II bands were detected at 1655 and 1535 cm^{-1}, respectively. However, a very strong ^{13}C amide I band was also detected at 1625 cm^{-1} in the IP spectrum in **Figure 3.7**. The peak at 1625 cm^{-1} cannot be assigned to the β-sheets conformation because no signal of β-sheets was detected in the CD result (**Figure 1.6**) mentioned above. In addition, it has been reported that the position of the ^{13}C amide I band may be ~30-40 cm^{-1} lower than that of the regular amide I band of α-helix in the same environment.[20] Therefore, the position at 1625 cm^{-1} shows that the 93G is also in α-helical conformation in the LB film. In addition, the ^{13}C amide I band in the IP spectrum is even stronger than the regular amide I band at 1655 cm^{-1}, which is the absorption sum of all the other thirty-four residues in the sequence of α-syn (61-95). Such an intense ^{13}C amide I band suggests a very small tilt angle (i.e., parallel orientation) of the ^{13}C amide I transition moment.

The out-of-plane (OP) spectrum which is the bottom curve in **Figure 3.7** correlates with the IP spectrum and confirms this conclusion. The regular amide I and II bands were also detected in the OP spectrum. The regular amide I band feature shows splitting at 1659 and 1645 cm^{-1}, possibly stemming from the coupling between the regular and the ^{13}C amide I transition moment.[6] More importantly, the ^{13}C amide I band at 1625 cm^{-1} was not detected

in the OP spectrum, even though the ^{13}C label does exist at position 93G. According to the selection rule of pMAIRS shown in Equation 1, the tilt angle of the ^{13}C amide I transition moment at 93G is ~0 º.

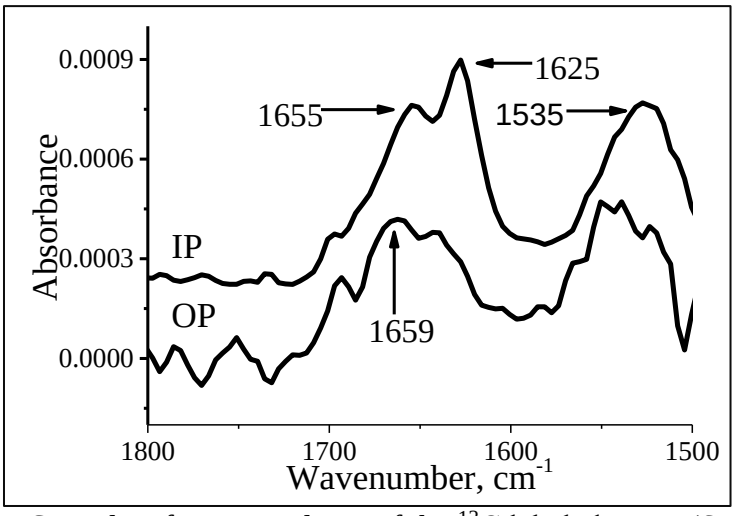

Figure 3.7 pMAIRS results of LB monolayer of the ^{13}C labeled α-syn (61-95) at position 93G transferred at 6 mN/m after the surface pressure was held for 2 hours.

3.5 pMAIRS results of ^{13}C labeled α-Syn (61－95) at 93G held at 6 mN/m for 15 Minutes.

Figure 3.8 below shows the pMAIRS results of the LB monolayer of the ^{13}C labeled α-syn (61-95) at position 93G transferred at 6 mN/m after the surface pressure was held for 15 minutes. As for IP result, all the peaks (such as 1655 cm^{-1} for regular amide I band, 1624 cm^{-1} for ^{13}C amide I band, and 1545 cm^{-1} for amide II band) in **Figure 3.7** were also detected in **Figure 3.8.** However, the intensity of the ^{13}C amide I band in **Figure 3.8**

is lower than that in **Figure 3.7**. Since the only difference of the LB monolayers prepared for **Figure 3.7** and **3.8** is the holding time, it can be concluded that the shorter holding time of 15 minutes make the ^{13}C amide I band at 93G more tilted to the interface at 93G. The OP result in **Figure 3.8** also consistent with the conclusion from the IP result. Although regular amide I and II bands were also detected at 1655 and 1550 cm^{-1}, respectively, the ^{13}C amide I band disappeared in **Figure 3.7** was present in the OP result of **Figure 3.8**. This shows the more tilted orientation of the ^{13}C amide I band at 93G with 15 minutes holding time.

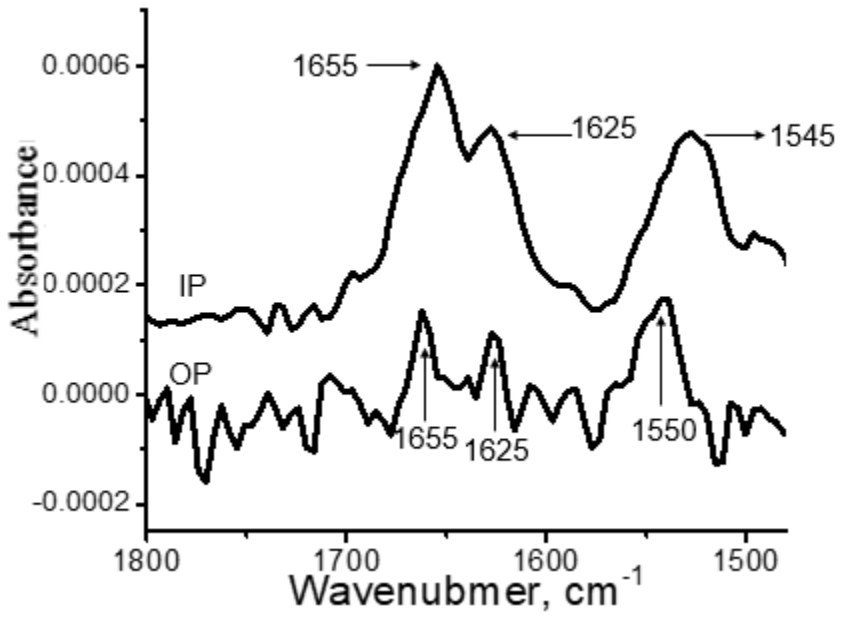

Figure 3.8 pMAIRS results of LB monolayer of the ^{13}C labeled α-syn (61-95) at position 93G transferred at 6 mN/m after the surface pressure was held for 15 minutes.

CHAPTER 4

DISCUSSION AND FUTURE PERSPECTIVE

4.1 Discussion

Raman spectroscopy is found to be less effective in the determination of the orientation of α-syn (57－102) in monolayer as the single peak observed in **Figure 3.4** is the signal from silicon wafer. To obtain useful signals, there is need for an extended spectral acquisition period. On the other hand, pMAIRS prove to be effective in determining the conformation as well as orientation of α-syn (61 － 95) monolayer. Additionally, it is shown that different holding time affects the orientation of α-syn (61－95) monolayer. When the LB monolayer of α-syn (61－95) held at 6 mN/m for 2 hours shown in **Figure 3.6**, the tilted angle of amide I band is 21.2 °, while that held for only 15 minutes was 32.2 °. The longer holding time results in the axis of the α-helix in the monolayer becoming more parallel due to the decreased titled angle as shown in **Figure 4.1** below.

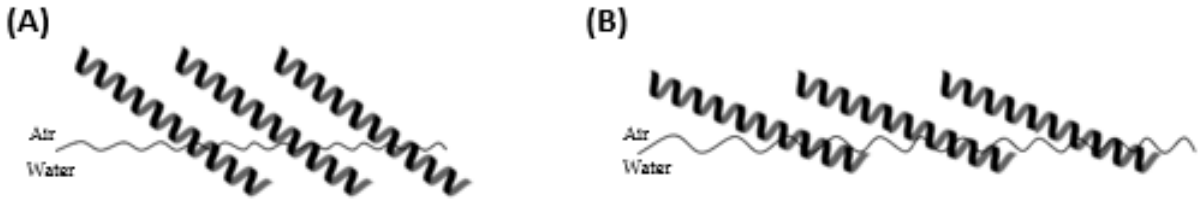

Figure 4.1. Tilt angle of amide I band (A) 32.2 ° and (B) 21.2 °

To address the orientation change of specific residues under various holding time, ^{13}C isotope label has been introduced into the sequence of α-syn (61－95) at the glycine at position 93 (i.e., 93G) because it was reported, that the biophysical behavior of residues near the sequence's terminus may vary from that of residues in the middle of the sequence in terms of conformation and orientation.[27] Therefore, the glycine at position 93 serves as a proof-of-principle example as it is close to the C-terminus of the sequence. As mentioned above, the critical information for α-helical membrane peptides/proteins at the interface is the orientation of its axis. Therefore, it is important to calculate the tilt angle of the axis based on the amide I transition moment. The ^{13}C amide I transition moment is mainly produced by the stretching mode of ^{13}C labeled backbone C=O, which was reported to be roughly parallel to the axis of the residue.[15] Together with the fact that the α-helix of α-syn (61－95) molecules may spin easily around the axis in the Langmuir monolayer at the interface,[15] the tilt angle of the axis at residue 93G may be equal to that of the ^{13}C amide I transition moment, namely, ~0 º when the monolayer was transferred after surface pressure held at 6 mN/m for 2 hours.

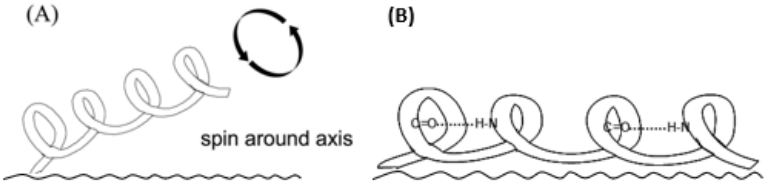

Figure 4.2. (A). Model of α-helix spinning around its axis at the air-water interface and (B) Backbone carbonyl of α-helix parallel to the interface.

4.2 Future perspective

As shown in **Figure 3.6**, the tilted angle of the amide I band (or even ^{13}C amide I band in **Figure 3.8**) can be quantitatively evaluated by pMAIRS even in monolayer structure. Then, what is the tilted angle of the ^{13}C amide I band for the monolayer prepared at 6 mN/m for 15 minutes shown in **Figure 3.8**? Notice that the ^{13}C amide I band overlaps with the regular amide I band in **Figure 3.8** (especially in the IP result). Therefore, the peak intensity of ^{13}C amide I band in the IP result (i.e., A_{IP}) cannot be calculated accurately for Equation 1 shown in the Introduction and discussed above. Thus, the tilted angle cannot be quantitatively determined here. To resolve this problem, $^{13}C=^{18}O$ will be considered in future research because ^{18}O will further downshift the amide I band around 1600 cm^{-1} for α-helix so that the $^{13}C=^{18}O$ amide I band will not overlap with the regular amide I band. Despite acquiring the spectra over nine thousand scans and accounting for water vapor, the OP signal in **Figure 3.8** is rather weak and will be improved on in subsequent research.

REFERENCES

1. Sun, P. D., Foster, C. E., & Boyington, J. C. (2004). Overview of protein structural and functional folds. *Curr Protoc Protein Sci*, *Chapter 17*(1), Unit 17.11.
2. Gromiha, M. M. (2010). Chapter 1 - Proteins. In M. M. Gromiha (Ed.), *Protein Bioinformatics* (pp. 1-27). Singapore: Academic Press.
3. Hu, Y., Cheng, K., He, L., Zhang, X., Jiang, B., Jiang, L., . . . Liu, M. (2021). NMR-BasedMethods for Protein Analysis. *Analytical Chemistry, 93*(4), 1866-1879.
4. Mishra, S., Demo, G., Koc?a, J., & Wimmerová, M. (2012). In Silico Engineering of Proteins That Recognize Small Molecules. In.
5. Krogh, A., Larsson, B., Heijne, G., & Sonnhammer, E. L. L. (2001). Predicting transmembrane protein topology with a hidden Markov model: Application to complete genomes. *J. Struct. Biol., 305*, 567-580.
6. Manor, J., Arbely, E., Beerlink, A., Akkawi, M., & Arkin, I. T. (2014). Use of isotope-edited FTIR to derive a backbone structure of a transmembrane protein. *J. PHys. Chem. Lett., 5*, 2573-2579.
7. Cook, G. A., & Opella, S. J. (2010). NMR studies of membrane proteins. *Methods Mol Biol, 637*, 263-275. doi:10.1007/978-1-60761-700-6_14.
8. Opella, S. J., & Marassi, F. M. (2004). Structure determination of membrane proteins by NMR spectroscopy. *Chem Rev, 104*(8), 3587-3606. doi:10.1021/cr0304121.
9. Meade, R. M., Fairlie, D. P., & Mason, J. M. (2019). Alpha-synuclein structure and Parkinson's disease – lessons and emerging principles. *Molecular Neurodegeneration, 14*(1), 29.
10. Wang, C., Zhao, C., Li, D., Tian, Z., Lai, Y., Diao, J., & Liu, C. (2016). Versatile Structures of α-Synuclein. *Frontiers in Molecular Neuroscience, 9*.
11. Kim, W. S., Kågedal, K., & Halliday, G. M. (2014). Alpha-synuclein biology in Lewy body diseases. *Alzheimer's Research & Therapy, 6*(5), 73.
12. Breydo, L., Wu, J. W., & Uversky, V. N. (2012). A-synuclein misfolding and Parkinson's disease. *Biochim Biophys Acta, 1822*(2), 261-285.
13. Han, H., Weinreb, P. H., & Lansbury, P. T., Jr. (1995). The core Alzheimer's peptide NAC forms amyloid fibrils which seed and are seeded by beta-amyloid: is NAC a common trigger or target in neurodegenerative disease? *Chem Biol, 2*(3), 163-169.

14. Zhang, G., Xia, Y., Wan, F., Ma, K., Guo, X., Kou, L., . . . Wang, T. (2018). New Perspectives on Roles of Alpha-Synuclein in Parkinson's Disease. *Frontiers in Aging Neuroscience, 10*.

15. Fink, A. L. (2006). The aggregation and fibrillation of a-synuclein. *Acc. Chem. Res., 39*, 628-634.

16. Qin, Z., Hu, D., Han, S., Hong, D., & Fink, A. L. (2007). Role of different regions of a-synuclein in the assembly of fibrils. *Biochemistry, 46*, 13322-13330.

17. Wang, C., Shah, N., Thakur, G., Zhou, F., & Leblanc, R. M. (2010). a-Synuclein in a-helical conformation at the air-water interface: Implication of conformation and orientation changes during its accumulation/aggregation. *Chem. Commun., 46*, 6702-6704.

18. Sharma, S. K., Seven, E. S., Micic, M., Li, S., & Leblanc, R. M. (2018). Surface Chemistry and Spectroscopic Study of a Cholera Toxin B Langmuir Monolayer. *Langmuir, 34*(7), 2557-2564.

19. Dziri, L., Desbat, B., & Leblanc, R. M. (1999). Polarization modulated FT-IR spectroscopy studies of acetylcholinesterase secondary structure at the air-water interface. *J. Am. Chem. Soc., 121*, 9618-9625.

20. Yang, G., Dong, Y., Gong, K., Jiang, W., Kwon, E., Wang, P., . . . Zhao, N. (2005). Reduced synaptic vesicle density and active zone size in mice lacking amyloid precursor protein (APP) and APP-like protein 2. *Neurosci. Lett., 384*, 66-71.

21. Hasegawa, T. (2017). *Quantitative Infrared spectroscopy for understanding of a condensed matter*: Springer

22. Decatur, S. M. (2006). Elucidation of residue-level structure and dynamics of polypeptides via isotopp-edited infrared spectroscopy. *Acc. Chem. Res., 39*, 169-175.

23. Li, S., Combs, J. D., Alharbi, O. E., Kong, J., Wang, C., & Leblanc, R. M. (2015). The ^{13}C amide I band is still sensitive to conformation change when the regular amide I band cannot be distinguished at the typical position in H_2O. *Chem. Commun., 51*, 12537-12539.

24. Wang, C., Shah, N., Thakur, G., Zhou, F., & Leblanc, R. M. (2010). a-Synuclein in a-helical conformation at the air-water interface: Implication of conformation and orientation changes during its accumulation/aggregation. *Chem. Commun., 46*, 6702-6704.

25. Wang, C., Sharma, S. K., Olaluwoye, O. S., Alrashdi, S. A., Hasegawa, T., & Leblanc, R. M. (2019). Conformation change of α-synuclein (61 - 95) at the air-water interface and quantitative measurement of the tilt angle of the axis of its α-helix by multiple angle incidence resolution spectroscopy. *Colloids and Surfaces B: Biointerfaces, 183*, 110401.

26. Sharma, S. K., Seven, E. S., Micic, M., Li, S., & Leblanc, R. M. (2018). Surface Chemistry and Spectroscopic Study of a Cholera Toxin B Langmuir Monolayer. *Langmuir, 34*(7), 2557-2564.

27. Li, S., Sneha, P., Keith, J. D., Wang, C., & Leblanc, R. M. (2014). Determination of geometry of a-helical model peptide by ^{13}C isotope edited FTIR in H_2O by ATR technique. *Chem. Commun., 50*, 3931-3933.

28. Flynn, J. D., Jiang, Z., & Lee, J. C. (2018). Segmental ^{13}C-labeling and Raman microspectroscopy of a-synuclein amyloid formation. *Angew. Chem. Int. Ed., 57*, 17069-17072.

29. Oladepo, S. A., Xiong, K., Hong, Z., Asher, S. A., Handen, J., & Lednev, I. K. (2012). UV resonance Raman investigations of peptide and protein structure and dynamics. *Chem. Rev., 112*, 2604-2628.

30. Lee, P. C., & Meisel, D. (1982). Adsorption and surface-enhanced Raman of dyes on silver and gold sols. *The Journal of Physical Chemistry, 86*(17), 3391-3395. doi:10.1021/j100214a025.